SYNAPSE 30:380–392 (1998)

Test–Retest Variability of Serotonin 5-HT_{2A} Receptor Binding Measured With Positron Emission Tomography and [^{18}F]Altanserin in the Human Brain

GWENN S. SMITH,[1,2]* JULIE C. PRICE,[2] BRIAN J. LOPRESTI,[2] YIYUN HUANG,[2] NORMAN SIMPSON,[2] DANIEL HOLT,[2] N. SCOTT MASON,[2] CAROLYN CIDIS MELTZER,[1,2] ROBERT A. SWEET,[1] THOMAS NICHOLS,[2] DONALD SASHIN,[2] AND CHESTER A. MATHIS[2]

[1]*Department of Psychiatry, Western Psychiatric Institute and Clinic, University of Pittsburgh School of Medicine, Pittsburgh, Pennsylvania*

[2]*Department of Radiology, University of Pittsburgh School of Medicine, Pittsburgh, Pennsylvania*

KEY WORDS positron emission tomography (PET); serotonin receptor; 5-HT_{2A}; imaging

ABSTRACT The role of serotonin in CNS function and in many neuropsychiatric diseases (e.g., schizophrenia, affective disorders, degenerative dementias) support the development of a reliable measure of serotonin receptor binding in vivo in human subjects. To this end, the regional distribution and intrasubject test–retest variability of the binding of [^{18}F]altanserin were measured as important steps in the further development of [^{18}F]altanserin as a radiotracer for positron emission tomography (PET) studies of the serotonin 5-HT_{2A} receptor. Two high specific activity [^{18}F]altanserin PET studies were performed in normal control subjects (n = 8) on two separate days (2–16 days apart). Regional specific binding was assessed by distribution volume (DV), estimates that were derived using a conventional four compartment (4C) model, and the Logan graphical analysis method. For both analysis methods, levels of [^{18}F]altanserin binding were highest in cortical areas, lower in the striatum and thalamus, and lowest in the cerebellum. Similar average differences of 13% or less were observed for the 4C model DV determined in regions with high receptor concentrations with greater variability in regions with low concentrations (16–20%). For all regions, the absolute value of the test–retest differences in the Logan DV values averaged 12% or less. The test–retest differences in the DV ratios (regional DV values normalized to the cerebellar DV) determined by both data analysis methods averaged less than 10%. The regional [^{18}F]altanserin DV values using both of these methods were significantly correlated with literature-based values of the regional concentrations of 5-HT_{2A} receptors determined by postmortem autoradiographic studies ($r^2 = 0.95$, $P < 0.001$ for the 4C model and $r^2 = 0.96$, $P < 0.001$ for the Logan method). Brain uptake studies in rats demonstrated that two different radiolabeled metabolites of [^{18}F]altanserin (present at levels of 3–25% of the total radioactivity in human plasma 10–120 min postinjection) were able to penetrate the blood–brain barrier. However, neither of these radiolabeled metabolites bound specifically to the 5-HT_{2A} receptor and did not interfere with the interpretation of regional [^{18}F]altanserin-specific binding parameters obtained using either a conventional 4C model or the Logan graphical analysis method. In summary, these results demonstrate

Contract grant sponsor: National Institutes of Health; Contract grant numbers: MH49936, MH57078, MH54715, MH01153, MH52247 (Mental Health Clinical Research Center for the Study of Late Life Mood Disorders), MH49815 (Center for Functional Brain Imaging), RR00056 (General Clinical Research Center); Contract grant sponsor: the National Alliance for Research in Schizophrenia and Depression (NARSAD, Young Investigator Award to GSS).

*Correspondence to: Gwenn Smith, Ph.D., PET Facility, PUH B-938, University of Pittsburgh School of Medicine, 200 Lothrop Street, Pittsburgh, PA 15213. E-mail: gsmith@rad.arad.upmc.edu

Received 24 May 1997; Accepted 7 March 1998

that the test–retest variability of [^{18}F]altanserin-specific binding is comparable to that of other PET radiotracers and that the regional specific binding of [^{18}F]altanserin in human brain was correlated with the known regional distribution of 5-HT$_{2A}$ receptors. These findings support the usefulness of [^{18}F]altanserin as a radioligand for PET studies of 5-HT$_{2A}$ receptors. **Synapse 30:380–392, 1998.**

INTRODUCTION

The neuroanatomic organization of the serotonin system implicates a significant neuromodulatory role for serotonin. The cell bodies of origin of the serotonergic projections are located in the brainstem and have been subdivided into nine nuclear groups (Dahlstrom and Fuxe, 1984; Azmitia and Gannon, 1986). These nuclear groups provide diffuse, serotonergic innervation to the central nervous system (CNS), particularly to limbic and paralimbic areas (e.g., hippocampus, amygdala, temporal cortex) and to primary sensory areas (e.g., calcarine cortex, superior temporal gyrus, post-central gyrus, nuclei of the amygdala, and areas within the entorhinal cortex related to olfaction) (Steinbusch, 1981; Parent et al., 1981). Importantly, projections have been demonstrated from the serotonergic cell bodies (dorsal and medial raphe nuclei) to the cell bodies of origin of dopaminergic (substantia nigra and ventral tegmental area), cholinergic (nucleus basalis of Meynert, pedunculopontine nuclei), and noradrenergic (locus coerleus) systems (Jones and Cuello 1989; Van Bockstaele et al., 1994; Herregodts et al., 1991). Neurophysiologic studies also support the ability of serotonin to modulate other neurotransmitter systems (Benloucif et al., 1993; Hirano et al., 1995). There is considerable diversity of the serotonin receptor system in that at least 14 subtypes of the serotonin receptor have been identified (reviewed by Peroutka, 1994; Hoyer et al., 1994). The receptor subtypes that are the best characterized both pharmacologically and physiologically are those of the 5-HT$_1$ (5-HT$_{1A}$, 5-HT$_{1B}$, 5-HT$_{1D}$), 5-HT$_2$ (5-HT$_{2A}$, 5-HT$_{2B}$, and 5-HT$_{2C}$), and 5-HT$_3$ receptor families. Other receptor subtypes have been identified as well (5-HT$_4$, 5-HT$_5$, 5-HT$_6$, and 5-HT$_7$).

Advances in radiotracer chemistry have led to the development of imaging agents that can be used with positron emission tomography (PET) to visualize different aspects of the serotonin system (e.g., serotonin synthesis rate, serotonin reuptake site, 5-HT$_{1A}$, and 5-HT$_{2A}$ receptors) in vivo in the nonhuman primate and human brain (e.g., Diksic et al., 1990; Suehiro et al., 1993; Mathis et al., 1994, 1996; Blin et al., 1988; Lemaire et al., 1991). The potential use of many of these radiotracers in humans is limited by low ratios of specific to nonspecific binding and lack of selectivity for serotonergic versus other monoamine receptors (reviewed by Frost, 1990; Pike, 1995). A major focus of radiotracer development has been the 5-HT$_{2A}$ receptor, and the report of the synthesis and binding characteristics of [^{18}F]altanserin in the rat by Lemaire et al. (1991) represented a promising 5-HT$_{2A}$ radiotracer for potential use in human PET studies. In particular, [^{18}F]altanserin demonstrated relatively high ratios of specific to nonspecific binding and considerable selectivity for 5-HT$_{2A}$ receptors. Altanserin binds with greatest affinity to the 5-HT$_{2A}$ receptor, and demonstrates a lower affinity in vitro for α_1 and D_2 sites (K_i = 0.13 nM, 4.55 nM, and 62 nM, respectively; Leysen, 1989, 1990). In addition, altanserin binds with much greater affinity to the 5-HT$_{2A}$ receptor compared to the other serotonin receptor subtypes (5-HT$_{2C}$ K_i = 40 nM; 5-HT$_{1A}$ K_i = 1,570 nM; 5-HT$_{1B}$ K_i > 1,000 nM; Leysen, 1990). The initial human PET studies of [^{18}F]altanserin demonstrated the binding distribution and displacement of the radioligand following ketanserin administration (Biver et al., 1994; Sadzot et al., 1995).

The purpose of the present study was to further characterize [^{18}F]altanserin as a radiotracer for the 5-HT$_{2A}$ receptor based on 1) the correspondence between the regional distribution of [^{18}F]altanserin binding measured in vivo using PET imaging and the localization of 5-HT$_{2A}$ binding sites determined by literature-based in vitro autoradiographic studies in human postmortem brain tissue, and 2) the intrasubject test–retest variability of [^{18}F]altanserin binding in studies performed on two different days.

MATERIALS AND METHODS

Subjects

Subjects underwent medical (toxicology screening and laboratory testing) and psychiatric screening prior to PET imaging. Subject exclusion was based on personal or family history (first or second degree relatives) or current psychiatric or neurologic illness. Subjects were also excluded for significant medical illness or use of prescription or over-the-counter medications with CNS effects (e.g., antihistamines and other common cold medications) within the previous month. Following a complete description of the study to the subjects, written informed consent was obtained. The protocol and consent forms were approved by the University of Pittsburgh School of Medicine Biomedical Institutional Review Board and Human Studies Subcommittee/ Radioactive Drug Research Committee. Eight subjects (four male and four female) with a mean age of 22 ± 3.8 years were studied. The demographics for the subject sample are shown in Table I.

TABLE I. Demographic data

Subject number	Gender	Age (yrs)	Interval between studies (days)
1	Female	21	2
2	Female	19	2
3	Female	18	2
4	Female	21	16
5	Male	24	2
6	Male	29	2
7	Male	25	2
8	Male	22	6

MR imaging

All subjects underwent magnetic resonance (MR) imaging scans prior to the first PET study for region of interest (ROI) localization. The MR scans were performed with a Signa 1.5 Tesla scanner (GE Medical Systems, Milwaukee, WI). A T1-weighted MR pulse sequence was used for co-registration with the PET scans with the following parameters: TE = 18, TR = 400, NEX = 1 (3 mm slice thickness/interleaved). In preparation for registration with the PET scans, the MR images were edited to remove the extracerebral tissues (e.g., scalp) as described by Woods et al. (1993), using ANALYSE software (Mayo Software, Rochester, MN).

PET imaging

[^{18}F]Altanserin was synthesized as described previously by Lemaire et al. (1991). The average injected dose was 9.6 ± 0.6 mCi (range 8.5–11.0 mCi) and the average specific activity was 1.55 ± 0.60 Ci/μmol. All of the PET scans were performed at the same time of day. After placement of a catheter into either the left or right radial artery and an intravenous line in an antecubital vein in the opposite arm, the subject was positioned in an ECAT 951R/31 PET scanner (Siemens/CTI, Inc, Knoxville, TN). A softened thermoplastic mold with holes for the eyes, nose, and ears was fitted closely around the head and was attached to the head holder to help prevent head movement. A transmission scan (Huang et al., 1979) was obtained using rotating rods of ^{68}Ge/^{68}Ga with electronic windowing to minimize the detection of scatter. After the transmission scan, [^{18}F]altanserin was injected intravenously. Scanning began immediately upon injection of the radiotracer and continued for 121 min. The 121-min PET study duration was chosen to permit evaluation of the stability of the DV measure at later times (e.g., > 90 min) when radioligand dissociation and tissue clearance would be more evident. The scanning protocol involved six scanning frames of 20 sec followed by two frames of 30 sec, one frame of 60 sec, two frames of 90 sec, three frames of 3 min, one frame of 5 min, and ten frames of 10 min. To determine the reliability of measuring [^{18}F]altanserin-specific binding using a shorter scan protocol, analyses were also performed using only 90 min of data, and these results were compared to those obtained using 121 min.

Plasma assays

The total radioactivity concentration in plasma was determined throughout the study from 38 hand-drawn 0.5 mL arterial blood samples obtained about every 6 sec for the first 2 min and then with reduced frequency to every 10 min. The blood samples were centrifuged and plasma was separated (0.2 mL) and counted in a gamma counter (Packard Cobra 5003, Meriden, CT).

Plasma samples were also obtained at 2, 10, 30, 60, 90, and 120 min postinjection and used to determine the fraction of unmetabolized [^{18}F]altanserin in plasma. Approximately 2 mL of arterial blood were withdrawn and centrifuged. Plasma (0.5 mL) was added to a solution (20 mL) of 50 mM acetic acid and 1 μM carrier (nonradioactive) altanserin and eluted through a Waters C18 SepPak Light cartridge. Radioactivity was quantitatively retained on the cartridge (>98%), and the cartridge was sequentially eluted with aqueous 0.1% triethylamine (5 mL), water (5 mL), and methanol (1.5 mL). Methanol removed more than 98% of the radioactivity from the cartridge, while the aqueous triethylamine and water washes removed less than 2% of the radioactivity. The methanol eluent was passed through a Millipore HV syringe filter and injected onto a Waters analytical μBondapak C18 HPLC column. The column was eluted with a mixture of 23% acetonitrile and 77% aqueous buffer (0.3 M acetic acid/0.03 M ammonium acetate, pH 5). Eluent fractions (2 mL) were collected and counted in a gamma counter. The fraction of unmetabolized [^{18}F]altanserin (of the total radioactivity in the plasma) was determined as a function of time, and a multi-exponential function was fit to these data. This equation was used to estimate the fraction of [^{18}F]altanserin in plasma at each plasma curve timepoint (metabolite correction factor). The concentration of unmetabolized [^{18}F]altanserin in plasma (input function) was determined by performing a point-by-point multiplication of the total measured plasma radioactivity concentration by the corresponding metabolite correction factor.

Image analysis

The [^{18}F]altanserin PET studies acquired on two separate days were aligned to each other and then to the MRI scan using the automated image registration (AIR) algorithm (Woods et al., 1992, 1993). In a comparison of several methods for MRI/PET alignment, the AIR algorithm was shown to be the superior method (Strother et al., 1994). The early dynamic frames from 0 to 21 min (first 15 frames) were summed to create an image that largely reflected cerebral blood flow, since AIR has been validated with blood flow images acquired with [^{15}O]water. Using the symmetry principle of Minoshima et al. (1992), AIR software was used to

center the Day 1 image, and the second summed PET scan was aligned to the first summed PET scan. The AIR alignment matrix generated to align the two summed PET scans was then applied to the individual frames of each of the two PET scans. The MRI scan was aligned and resliced to yield MR images in the same spatial orientation as the PET scans.

All regions of interest (ROIs) were drawn on the resliced MR dataset of each subject and applied to the PET datasets. ROIs were identified for anterior cingulate gyrus (ACG), prefrontal cortex (PFC), orbitofrontal cortex (OFC), mesial temporal cortex (MTC; amygdala/hippocampus), lateral temporal association cortex (LTC), striatum (STR; caudate and putamen), thalamus (THL), and cerebellum (CER). Decay-corrected tissue time–activity data were generated for each ROI.

Kinetic modeling analysis

In the present study, conventional tracer kinetic modeling methods were applied. The [^{18}F]altanserin data were analyzed using the Logan graphical analysis (Logan et al., 1990) and compartmental modeling, as recently described (Biver et al., 1994; Price et al., 1998). Linear three- and four-compartment models (3C and 4C) that corresponded to two and three tissue compartments were applied to the PET data using nonlinear least-squares curve-fitting methods. The cerebellar data were assumed to be a good approximation of the free concentration and nonspecific binding of [^{18}F]altanserin due to relatively low 5-HT$_{2A}$ receptor concentrations in this brain region (Pazos et al., 1987). For receptor-binding data, the 4C model was constrained using cerebellar parameter values (3C: K_1–k_4) that were assumed to reflect regional blood–brain barrier transport (K_1:k_2 ratio) and nonspecific binding (k_5 and k_6 fixed to cerebellar k_3 and k_4, respectively). The application of these constraints was based on the assumptions that the rates of bidirectional transport of [^{18}F]altanserin across the blood–brain barrier and that nonspecific binding are largely invariant in all brain tissues. The Logan slope and 4C model parameters provided specific binding estimates that corresponded to the regional radioligand distribution volume (DV, ml/ml) and distribution volume ratio (DV ratio: regional DV normalized to the cerebellar DV).

Radiolabeled metabolite analyses

Using HPLC analysis methods similar to those described above (eluent step gradient from 15% acetonitrile to 25% acetonitrile at 30 min and the balance aqueous 0.3 M acetic acid / 0.03 M ammonium acetate, pH 5 buffer), three major radiolabeled metabolites (≥3% of the plasma radioactivity at any time point) of [^{18}F]altanserin were found in human plasma, and the same three major metabolites of [^{18}F]altanserin were also found in the plasma and urine of baboons (Price et al., 1998). To date, the chemical structure of only one of the three radiolabeled metabolites has been conclusively identified (Lopresti et al., in press). To determine if these radiolabeled metabolites crossed the blood–brain barrier, each of the three major metabolites was isolated separately from the urine of baboons using semipreparative HPLC separation methods and injected intravenously via the tail-vein into three different groups of male Sprague-Dawley rats (n = 3–4 per group). The rats were killed either 2 min or 60 min after the injection of one of the radiolabeled metabolites; a blood sample was taken at the time of death and their brains were removed, dissected, counted, and weighed to determine the percent of the injected dose of radioactivity per gram (%ID/g) brain tissue in different brain regions (e.g., see Mathis et al., 1994, 1996, for in vivo rat brain uptake methods). Three other groups of rats were pretreated (i.v. tail-vein) with the potent and selective 5-HT$_{2A}$ antagonist SR 46349B (Rinaldi-Carmona et al., 1992; 3 mg/kg) 10 min prior to the injection of one of the three major isolated radiolabeled metabolites. For comparison, two other groups of rats were used as controls: one group received no blocking pretreatment and the other group was pretreated with SR 46349B (3 mg/kg) 10 min prior to the injection of [^{18}F]altanserin.

One of the major radiolabeled metabolites of [^{18}F]altanserin was identified as [^{18}F]altanserinol (Meuldermans et al., 1984), and this compound was synthesized (Mason et al., 1997) for in vitro binding studies. The ability of altanserin and altanserinol to inhibit [^{3}H]ketanserin binding to human 5-HT$_{2A}$ receptors expressed in Chinese hamster ovary (CHO) cells was examined. Binding assays over a range of 1×10^{-12} to 1×10^{-4} M competitor were conducted in triplicate in pH 7.4 Tris-HCl buffer using 0.34 nM [^{3}H]ketanserin incubated for 30 min with CHO cells maintained at 37°C. Nonspecific binding was determined using 1×10^{-6} M mianserin.

Correlations between in vivo and in vitro binding

To determine the correspondence of the regional binding distribution of [^{18}F]altanserin to the 5-HT$_{2A}$ receptor, correlations were performed between the receptor binding parameters (Logan and compartmental model DV values) and in vitro autoradiographic data obtained in postmortem human brain with [^{3}H]ketanserin (Pazos et al., 1987). The postmortem autoradiographic data of Pazos et al. indicated 5-HT$_{2A}$ receptor densities in a variety of substructures contained within the boundaries of the MR-based ROIs used to define the PET regions (e.g., values in each cortical layer I–VI). The limited resolution of the tomograph utilized in the PET imaging studies (about 7 mm) necessarily resulted in a volumetric average of these autoradiographically determined substructures. Therefore, the [^{3}H]ketan-

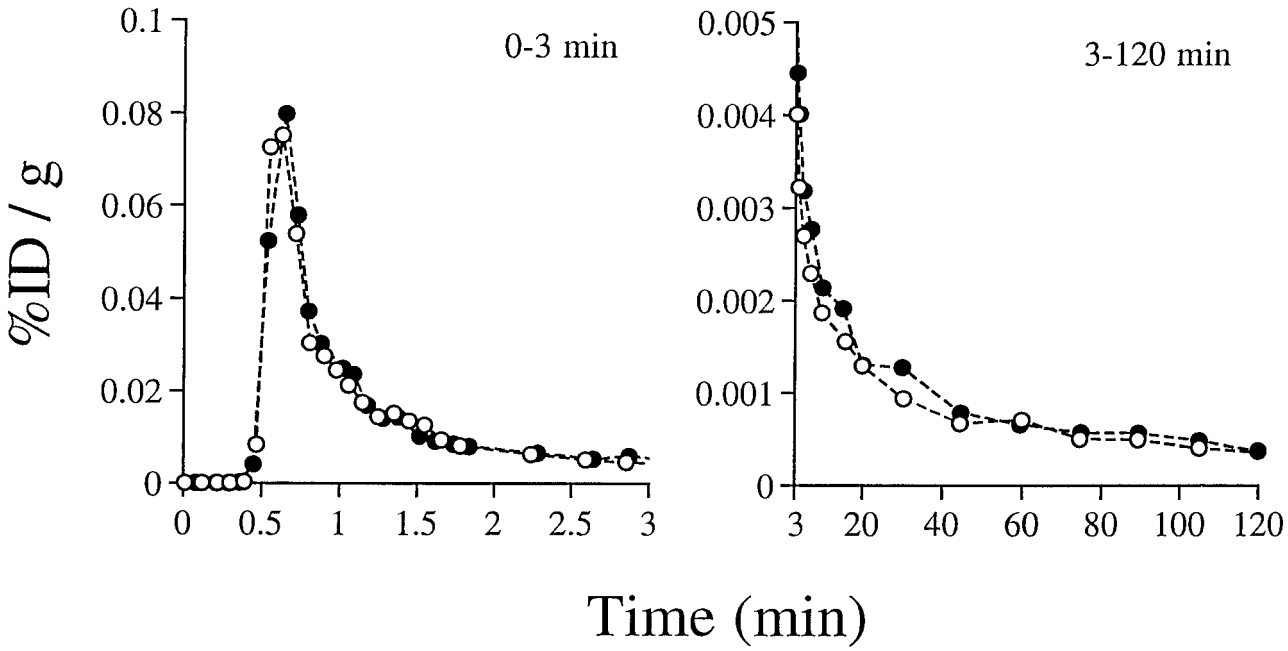

Fig. 1. The percent injected dose per gram (%ID/g) of [18F]altanserin in plasma over time is shown for the two study days for a typical subject (Day 1: open circles; Day 2: solid circles). The left graph displays the early (0–3 min) and the right graph the late (3–121 min) data.

TABLE II. Percent of unmetabolized [18F]altanserin in arterial plasma (± standard deviation; n = 8)

	2 min	10 min	30 min	60 min	90 min	120 min
Day 1	96.2 ± 1.0%	83.0 ± 4.6%	63.2 ± 8.9%	50.6 ± 10.2%	44.7 ± 10.3%	41.1 ± 10.3%
Day 2	95.2 ± 1.3%	81.0 ± 5.2%	62.7 ± 9.1%	50.9 ± 10.3%	44.5 ± 10.8%	40.0 ± 11.7%

serin binding densities in the various substructures reported by Pazos et al. were averaged and plotted against the PET-derived Logan and compartmental model DV values.

RESULTS

Plasma assays

An example of an [18F]altanserin arterial input function is shown in Figure 1 and the average amount of unmetabolized [18F]altanserin in arterial plasma 2–120 min postinjection is given in Table II. There were no significant intrasubject differences across the two studies in the percent of unchanged [18F]altanserin in plasma for any of the timepoints.

Kinetic modeling analysis

In the present study, the results of two conventional tracer kinetic methods that do not explicitly account for the passage of radiolabeled metabolites across the blood–brain barrier were compared. These analyses were deemed valid based on the in vivo experiments in rats and the in vitro binding studies that support the premise that radiolabeled metabolites of [18F]altanserin that cross the blood–brain barrier primarily contribute to nonspecific and free radioactivity concentrations in brain and do not specifically bind to the 5-HT_{2A} receptor (see below).

Examples of a time–activity curve for a representative subject for several brain regions (PFC, MTC, CER) for the Day 1 and Day 2 studies are shown in Figure 2, along with the compartmental model fit. The Logan graphical analyses of these data are presented in Figure 3. The mean regional DV and DV ratio values for the two data analysis methods for the Day 1 and Day 2 studies are shown in Tables III and IV, and the means of the absolute values of the intrasubject variability are shown in Table V. The subjects varied in the direction of change in specific binding, as some subjects showed an increase and some showed a decrease between the two days of study. The means of the absolute percent difference values are presented and this maximizes the mean variability reported. It is important to note that for both data analysis methods, comparable percent differences across regions with high and low levels of specific binding were observed.

The analyses of the 90-min datasets provided mean and variability measures for the regional DV and DV ratios that were in good agreement with the 121-min results for seven of eight subjects. The Day 1 90-min Logan DV values (and test–retest percent) for the PFC,

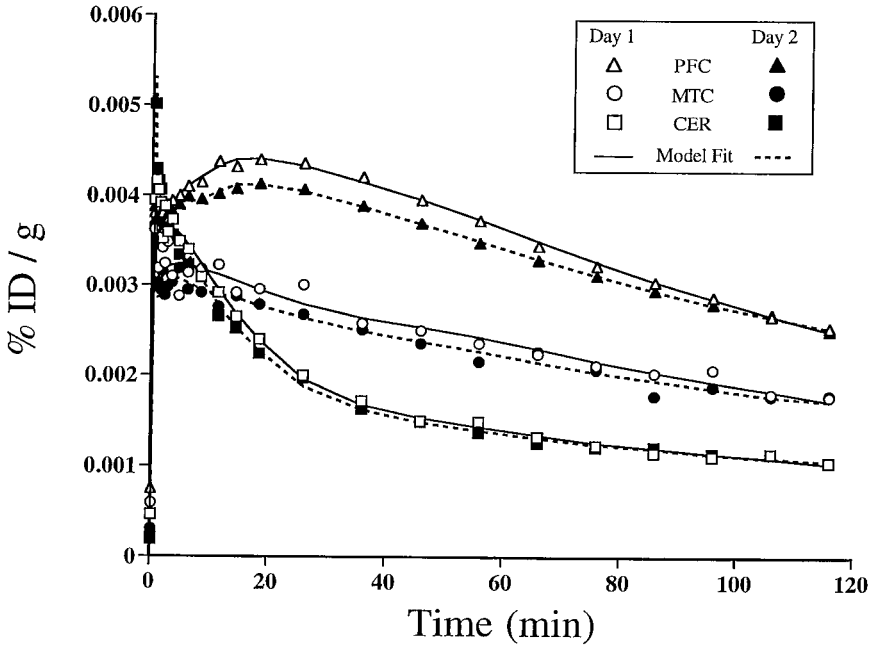

Fig. 2. PET time–activity data and the corresponding compartmental model curve fits are shown for the prefrontal cortex, mesial temporal cortex, and cerebellum for the Day 1 (solid line) and Day 2 (dashed line) studies of a representative subject. Clearance of radioligand from brain (radioligand reversibility) is evident for all regions.

MTC, and CER were: 3.0 ± 0.8 (11.0 ± 5.3%), 2.1 ± 0.5 (8.5 ± 5.1%), and 1.2 ± 0.3 (11.8 ± 5.1%) with corresponding PFC and MTC DV ratios (and test–retest percent) of: 2.4 ± 0.2 (3.2 ± 2.9%) and 1.7 ± 0.2 (5.2 ± 5.3%), respectively (n = 7). Similarly, the Day 1 90-min 4C and 3C model DV values (and test–retest percent) for the PFC, MTC, and CER were: 2.7 ± 0.8 (10.5 ± 5.7%), 1.9 ± 0.5 (11.0 ± 5.4%), and 1.1 ± 0.4 (17.7 ± 8.4%) with corresponding PFC and MTC DV ratios (and test–retest percent) of 2.7 ± 0.6 (13.0 ± 20.4%) and 1.9 ± 0.5 (10.2 ± 12.4%), respectively (n = 7). The analyses of the 90-min data for the eighth subject yielded Logan results that were consistent with the values of the other seven subjects listed above, while the compartmental model Day 2 DV was unusually unstable, yielding low estimates for the nonspecific dissociation rate constant that led to large 4C model DV values and test–retest differences much greater than were obtained using the full 121-min data as inputs for the compartmental model.

Figure 4 shows an example of the Day 1 and Day 2 [^{18}F]altanserin PET scans in which each pixel in the image represents the DV determined by the Logan graphical analysis method. A linear regression was performed using 13–121 min of time–activity PET data for each pixel. The corresponding pixel in a new image was assigned the regression slope value and in this manner Logan DV images were generated. The co-registered MRI scan is shown in the middle column. There is good correspondence between the [^{18}F]altanserin PET images and the regional 5-HT$_{2A}$ receptor density determined by [^{3}H]ketanserin binding studies in the postmortem human brain (Pazos et al., 1987).

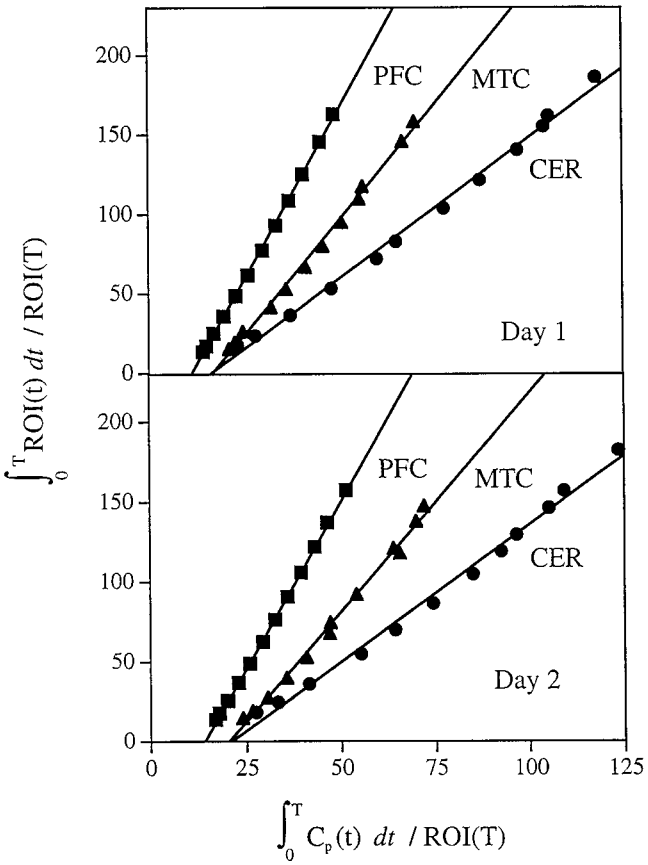

Fig. 3. Examples of the Logan results for the data presented in Figure 2. Linear regression analysis (solid line) was performed for data from 13 to 121 min, where ROI (T) is the radioactivity concentration in the ROI at time T and Cp(t) corresponds to the [^{18}F]altanserin plasma input function.

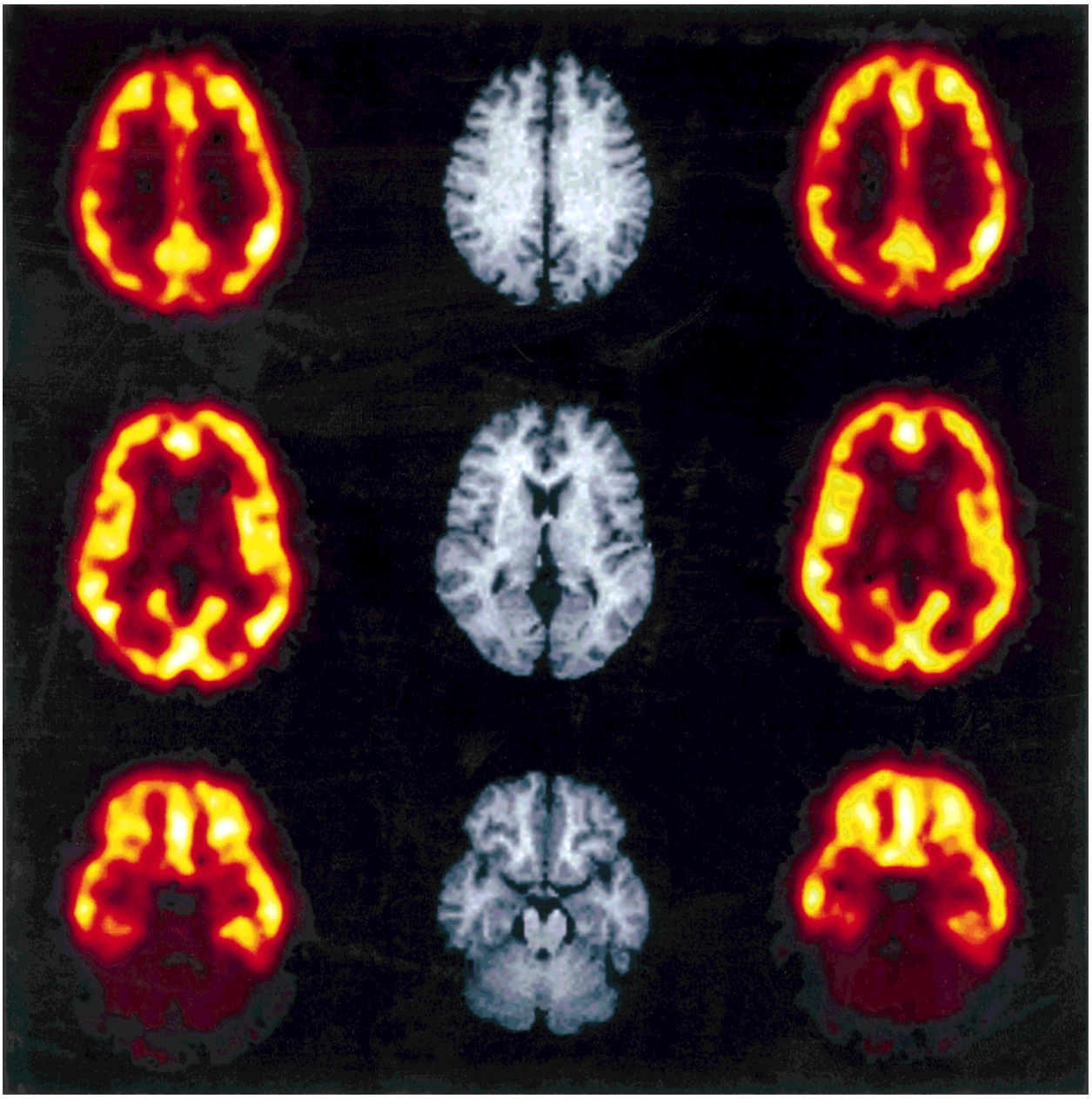

Fig. 4. Parametric images depicting the Logan derived DV for [^{18}F]altanserin on a pixel-by-pixel basis for a representative subject are shown. The images correspond to PET images acquired on the two study days (Day 1: left column; Day 2: right column) and to the co-registered MR image (center column). Three brain levels are displayed (centrum semiovale, striatum, and cerebellum). Note the relatively higher DV values in the cortical areas as compared to the striatum, thalamus, and cerebellum.

In vitro correlations

The correlations between the regional DVs derived by the Logan graphical analysis method and by the compartmental model for the ROIs plotted against the literature-based postmortem autoradiographic 5-HT$_{2A}$ receptor densities are shown in Figure 5. The Logan DV for the striatum is 1.76. The mean DVs derived by the graphical analysis and compartmental modeling approaches were equally well correlated with the 5-HT$_{2A}$ in vitro specific binding (Logan DV: $r^2 = 0.947$, $P < 0.001$ and compartmental model DV: $r^2 = 0.96$, $P < 0.001$).

To determine whether 90 min of data acquisition would provide specific binding parameters with good correspondence to the distribution of 5-HT$_{2A}$ binding sites, the 90-min DV values were also correlated with

*TABLE III. Intersubject variability for day 1 measures of regional [^{18}F]altanserin binding**

Method	Variable	CER	ACG	LTC	MTC	OFC	PFC	THL
Logan DV	Mean	1.33	3.32	3.24	2.21	3.34	3.20	1.69
	SD	0.38	0.96	0.97	0.63	1.09	0.94	0.54
Logan DV ratio	Mean	1.00	2.52	2.45	1.69	2.53	2.42	1.27
	SD	—	0.22	0.15	0.20	0.35	0.14	0.07
Model DV	Mean	1.47	3.51	3.43	2.39	3.54	3.38	1.86
	SD	0.61	1.16	1.19	0.85	1.32	1.17	0.77
Model DV ratio	Mean	1.00	2.56	2.44	1.70	2.53	2.42	1.28
	SD	—	0.80	0.50	0.28	0.63	0.53	0.15

*TABLE IV. Intersubject variability for day 2 measures of regional [^{18}F]altanserin binding**

Method	Variable	CER	ACG	LTC	MTC	OFC	PFC	THL
Logan DV	Mean	1.33	3.33	3.20	2.16	3.33	3.18	1.66
	SD	0.41	1.01	0.92	0.57	1.07	0.91	0.49
Logan DV ratio	Mean	1.00	2.53	2.44	1.67	2.54	2.42	1.26
	SD	—	0.24	0.14	0.20	0.36	0.14	0.04
Model DV	Mean	1.67	3.69	3.57	2.54	3.70	3.54	2.02
	SD	0.76	1.24	1.17	0.87	1.31	1.15	0.82
Model DV ratio	Mean	1.00	2.41	2.31	1.61	2.39	2.29	1.25
	SD	—	0.77	0.59	0.26	0.64	0.60	0.14

*TABLE V. Test-retest variability expressed as percent differences (absolute values) between day 1 and day 2 [^{18}F]altanserin binding**

Method	Variable	CER	ACG	LTC	MTC	OFC	PFC	THL
Logan DV	Mean	12.12	10.32	11.41	9.49	12.16	12.12	12.30
	SD	4.82	5.57	5.64	5.40	6.25	5.88	7.06
Logan DV ratio	Mean	1.00	2.08	3.93	4.78	2.01	3.65	4.55
	SD	—	1.63	2.71	5.04	1.68	2.96	3.77
Model DV	Mean	20.13	11.02	13.13	12.16	12.74	13.46	16.39
	SD	22.37	12.49	12.62	15.14	13.27	11.75	17.17
Model DV ratio	Mean	1.00	8.03	7.73	7.07	8.73	8.72	4.74
	SD	—	6.40	6.75	4.76	5.78	6.82	4.13

*For Tables III–V: n = 8; — = not applicable. Abbreviations: CER = cerebellum, ACG = anterior cingulate gyrus, LTC = lateral temporal cortex, MTC = mesial temporal cortex, OFC = orbitofrontal cortex, PFC = prefrontal cortex, THL = thalamus.

the in vitro 5-HT$_{2A}$ binding data. The 90-min correlations (Logan DV: $r^2 = 0.94$, $P < 0.001$ and compartmental model DV: $r^2 = 0.95$, $P < 0.001$) were comparable to those obtained using 121 min of data. The rank order of specific binding across regions was identical when the DVs were determined using either 90 or 121 min of data.

Radiolabeled metabolite analyses

A plot of the time course of the radiolabeled metabolites in human plasma is shown in Figure 6. The metabolites are numbered in the order of least (3) to most (1) polar. The rat brain uptake of [^{18}F]altanserin and the three major radiolabeled metabolites of [^{18}F]altanserin found in human plasma and shown in Figure 6 are summarized in Table VI. Representative rat brain regions are presented and include areas with known high (PFC, prefrontal cortex), moderate (HCP, hippocampus and STR, striatum), and low (CER, cerebellum) concentrations of 5-HT$_{2A}$ receptors (Pazos et al., 1985). Two of the metabolites readily crossed the blood–brain barrier, as the percent injected dose per gram of brain tissue (%ID/g) for metabolites 1 and 3 in the brain were about 0.4 and 0.1%/g, respectively, 2 min postinjection. These brain uptake values are similar to [^{18}F]altanserin at the 2-min timepoint, while the brain uptake of metabolite 2 was about 7-fold lower at 2 min and indicated that this metabolite did not readily cross the blood–brain barrier. At 60 min postinjection, nonspecifically bound and free radioactivity cleared from the cerebellum of the rats injected with [^{18}F]altanserin, and brain regions high in 5-HT$_{2A}$ receptors (e.g., PFC) demonstrated up to 5-fold higher concentrations of radioactivity compared to the cerebellum. Pretreatment of rats with the potent 5-HT$_{2A}$ antagonist SR 46349B 10 min prior to the injection of [^{18}F]altanserin resulted in the effective blockage of most of the specifically bound radioactivity in the PFC, while nonspecifically bound and free radioactivity concentrations in the cerebellum were relatively unchanged compared to untreated animals. In contrast, pretreatment of rats with SR 46349B 10 min prior to the injection of all three major radiolabeled metabolites of [^{18}F]altanserin re-

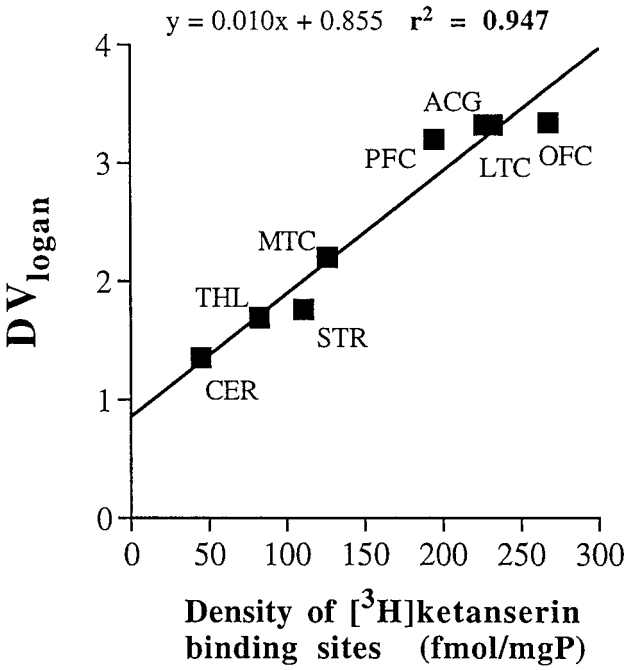

Fig. 5. The correlation between the regional [^{18}F]altanserin DV derived by the Logan graphical analysis method and the in vitro 5-HT$_{2A}$ receptor densities determined by autoradiography in postmortem brain with [^{3}H]ketanserin (Pazos et al., 1987). A significant correlation was obtained ($r^2 = 0.947$, $p < 0.001$).

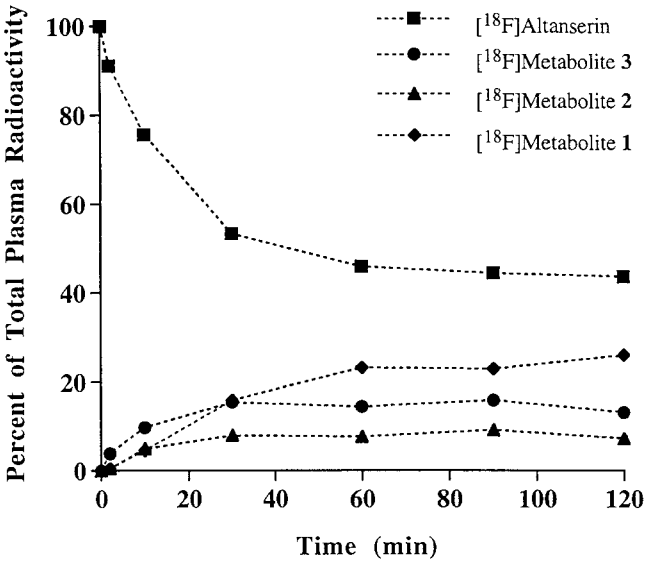

Fig. 6. The concentration of [^{18}F]altanserin and the three radiolabeled metabolites in plasma over time is shown for a typical subject. The metabolites are numbered in the order of least (3) to most (1) polar.

sulted in very little change in any brain region compared to untreated animals.

The in vitro binding studies demonstrated that the K_i for one of the major radiolabeled metabolites of altanserin (altanserinol) was 64 nM, while the K_i for altanserin was 0.51 nM. The 100-fold lower affinity of this metabolite relative to that of altanserin for the 5-HT$_{2A}$ receptor is consistent with negligible in vivo binding of the isolated radiolabeled metabolite to 5-HT$_{2A}$ receptors in the prefrontal cortex of rats described above. Based on the similarities of radioactivity concentrations in all brain regions of control and 5-HT$_{2A}$ antagonist pretreated rats discussed above, it is not likely that the other two major metabolites of [^{18}F]altanserin (metabolites 1 and 2) bind with high affinity to the 5-HT$_{2A}$ receptor.

DISCUSSION

The test–retest variability observed for [^{18}F]altanserin in the present study was comparable to that observed for other PET radiotracers for the measurement of glucose metabolic rates ([^{18}F]2-deoxy-2-fluoro-D-glucose; Bartlett et al., 1988), dopamine D_2 receptor binding ([^{11}C]raclopride; Volkow et al., 1993), dopamine turnover ([^{18}F]6-fluoro-DOPA; Pate et al., 1991), and muscarinic cholinergic receptor binding ([^{11}C]benztropine; Dewey et al., 1990). The comparable test–retest variability of [^{18}F]altanserin and that of other radiotracers is notable, given that the [^{18}F]altanserin studies were performed on different days and involved a longer scanning protocol (121 min vs. 20–60 min). Several subjects showed greater variability than others. These subjects were not distinguishable from the rest of the group in terms of demographic variables such as age and sex, the time interval between Day 1 and Day 2 scans, differences in rates of metabolism of [^{18}F]altanserin in plasma, or other parameters that would directly influence the calculation of the DV (e.g., K_1).

The DV ratio test–retest differences were greater for the compartmental analysis method as compared to the Logan graphical analysis. The DV ratios showed greater stability over time compared with the regional DVs for both analysis methods. Across all regions, the variability was reduced when the regional DVs were normalized to the cerebellum. The substantial improvement in reproducibility resulting from normalization to the cerebellum and the test–retest variability observed in the cerebellar DV values suggest that a large proportion of the variability was introduced by the free and nonspecific binding components.

The DV and DV ratio estimates were generally stable across methods and datasets (90 vs. 121 min). However, for one subject the tissue clearance was not well established by 90 min as compared to 121 min. For this case, the 90-min compartmental DVs were unstable relative to the Logan (90 min and 121 min) and the 121-min compartmental DVs. The results for this subject reinforce the fact that there are instances for which

*TABLE VI. Brain uptake of [^{18}F]altanserin and three major radiolabeled metabolites in rats**

^{18}F-Labeled compound	% ID/g at 2 min		% ID/g at 60 min		Blocked (3 mg/kg SR46349B) % ID/g at 60 min	
[^{18}F]Altanserin (control)	PFC	0.493 ± 0.237	PFC	0.502 ± 0.058	PFC	0.121 ± 0.021
	STR	0.380 ± 0.172	STR	0.258 ± 0.046	STR	0.149 ± 0.005
	HCP	0.299 ± 0.120	HCP	0.136 ± 0.027	HCP	0.107 ± 0.014
	CER	0.241 ± 0.063	CER	0.084 ± 0.004	CER	0.080 ± 0.008
	BLD	0.392 ± 0.203	BLD	0.165 ± 0.024	BLD	0.187 ± 0.039
[^{18}F]Metabolite 1	PFC	0.382 ± 0.126	PFC	0.298 ± 0.033	PFC	0.263 ± 0.059
	STR	0.425 ± 0.133	STR	0.388 ± 0.084	STR	0.299 ± 0.089
	HCP	0.362 ± 0.010	HCP	0.317 ± 0.007	HCP	0.248 ± 0.032
	CER	0.374 ± 0.088	CER	0.272 ± 0.023	CER	0.223 ± 0.025
	BLD	0.345 ± 0.078	BLD	0.263 ± 0.004	BLD	0.234 ± 0.008
[^{18}F]Metabolite 2	PFC	0.064 ± 0.053	PFC	0.020 ± 0.011	PFC	0.024 ± 0.008
	STR	0.055 ± 0.072	STR	0.008 ± 0.005	STR	0.018 ± 0.005
	HCP	0.029 ± 0.018	HCP	0.005 ± 0.004	HCP	0.020 ± 0.007
	CER	0.047 ± 0.003	CER	0.005 ± 0.005	CER	0.018 ± 0.013
	BLD	0.853 ± 0.085	BLD	0.041 ± 0.004	BLD	0.040 ± 0.008
[^{18}F]Metabolite 3 (Altanserinol)	PFC	0.128 ± 0.044	PFC	0.081 ± 0.051	PFC	0.049 ± 0.001
	STR	0.110 ± 0.065	STR	0.051 ± 0.021	STR	0.043 ± 0.001
	HCP	0.114 ± 0.059	HCP	0.057 ± 0.018	HCP	0.041 ± 0.001
	CER	0.121 ± 0.051	CER	0.044 ± 0.016	CER	0.033 ± 0.003
	BLD	0.200 ± 0.054	BLD	0.056 ± 0.020	BLD	0.040 ± 0.009

*PFC = prefrontal cortex; STR = striatum; HCP = hippocampus; CER = cerebellum; and BLD = blood.

the Logan method is clearly more stable than nonlinear least-squares curve-fitting methods (Logan et al., 1990). The data also indicate that [^{18}F]altanserin tissue clearance can be slower in some subjects and a longer scanning time might be required for stable compartmental DV estimates.

It is important to note that the DV ratios determined using either 90 or 121 min of data correlated equally well with the in vitro distribution of 5-HT$_{2A}$ receptors and that the rank order of binding of the DV ratios across regions was identical. This indicates that the [^{18}F]altanserin-specific binding measures can be determined using a shorter scanning protocol. The degree of clearance may be relevant to future studies using pharmacologic challenges to measure the competition between radiotracer binding and elevated endogenous serotonin concentrations. For these types of studies, the clearance half-time of the radiotracer from tissue has been shown to be an important determinant of parameter sensitivity to changes in endogenous neurotransmitter concentrations (Logan et al., 1991).

As described in the Introduction, the primary limitations of radiotracers previously developed to image the serotonin system (and in particular, the 5-HT$_{2A}$ receptor) are the relatively low ratios of specific to nonspecific binding due to high levels of nonspecific binding and the selectivity of these radiotracers for serotonin versus other monoamine receptors or transporters. Recently developed 5-HT$_{2A}$ antagonists that have a more selective pharmacologic profile than altanserin are currently being evaluated as potential PET radiotracers (e.g., [^{11}C]SR43936B (Tan et al., 1994); [^{18}F]RP 62203 (Besret et al., 1996); [^{11}C]MDL100,907 (Mathis et al., 1996)). The available data indicate that the ratios of specific to nonspecific binding in vivo for these radiotracers are the same as ([^{11}C]MDL100,907) or lower than ([^{11}C]SR43936B; [^{18}F]RP 62203) the ratios observed for [^{18}F]altanserin. In the future, the in vivo binding properties of these newer ligands will be compared with [^{18}F]altanserin to determine which of these radiotracers shows a greater sensitivity to pharmacologically induced changes in intracerebral endogenous serotonin concentrations. Relatively low levels of [^{18}F]altanserin-specific binding were observed in areas rich in D_2 receptors (e.g., STR) and α_1 receptors (e.g., STR and THL). As shown in Figure 5, DV values for [^{18}F]altanserin in the STR and THL were not disproportionately high relative to other brain regions known to contain low densities of α_1 and D_2 receptors. Thus, at the tracer doses used in these high specific-activity studies, [^{18}F]altanserin does not appear to significantly bind to α_1 and D_2 receptor subtypes. Another concern with the use of [^{18}F]altanserin is the evidence that radiolabeled metabolites of the radioligand enter the brain. Blocking studies in rats using the potent and selective 5-HT$_{2A}$ antagonist SR 46349B indicated this agent diminished the specific binding of [^{18}F]altanserin in brain regions known to contain high densities of 5-HT$_{2A}$ receptors and had little effect on regions known to contain low densities. Pretreatment was unable to significantly block radioactivity in the brain following the injection of the three major radiolabeled metabolites of [^{18}F]altanserin. In addition, in vitro binding studies of metabolite 3 (altanserinol) provide further support that this metabolite

does not bind with high affinity to the 5-HT_{2A} receptor. As shown in Table VI, two of the three major radiolabeled metabolites of [^{18}F]altanserin enter the brain to a significant degree. The brain uptake of metabolite 1 was similar to that of [^{18}F]altanserin at 2 min (about 0.4% ID/g), while the brain uptake of metabolite 3 was only about 0.1% ID/g. The initial concentrations of these two metabolites in the blood were zero at the time of [^{18}F]altanserin injection and metabolites 1 and 3 accounted for only about 20% and 10%, respectively, of the radioactivity in the plasma at 121 min following the injection of [^{18}F]altanserin (Fig. 6). Therefore, the areas under the curve (AUC) of metabolites 1 and 3 were more than 3-fold lower than that of [^{18}F]altanserin over the same time period. The higher brain uptake and larger AUC of metabolite 1 combine to make this species the predominant contributor to non-[^{18}F]altanserin radioactivity in brain tissue. However, the relatively low AUC of metabolite 1 compared to [^{18}F]altanserin indicates that the majority of nonspecifically bound and free radioactivity in the brain derives from [^{18}F]altanserin.

The importance of developing an in vivo measure of central serotonergic activity is supported by several lines of evidence. Consistent with the widespread distribution of serotonergic projections and the diversity of its receptor system, a role for the serotonin system has been implicated in a range of behaviors, including sleep, ingestive behavior, aggression, learning, and memory (McCarley and Hobson, 1975; Leibowitz and Shor-Poser, 1986; Brown and Linnoila, 1990; Spoont, 1992). The 5-HT_{2A} receptor, for example, has been localized to cortical GABA interneurons and cholinergic neurons of the basal forebrain, which suggests that this receptor subtype may be involved in disorders of these behaviors (Morilak et al., 1994a,b). In addition, the serotonin system has been implicated in many neuropsychiatric and neurodegenerative diseases, including major depressive disorder, obsessive compulsive disorder, schizophrenia, addictive disorders (alcoholism, cocaine abuse), normal aging, and Alzheimer's disease (e.g., Meltzer, 1991; Hollander et al., 1992; Stahl and Wets, 1987; Gross-Isseroff et al., 1990; Cross et al., 1986; Wolf and Kuhn, 1991). Previous studies of the serotonin system in these disease states have involved the examination of serotonin receptor number, biosynthetic enzymes and metabolites in postmortem brain tissue, the measurement of metabolites in plasma or in cerebrospinal fluid, or the assessment of changes in neuroendocrine hormones after serotonin agonist challenge (e.g., Arora and Meltzer, 1991; Mann et al., 1996; Kahn et al., 1993; Malone et al., 1993). These studies have provided evidence for serotonergic deficits in neuropsychiatric illness and, most importantly, have demonstrated that the response to treatment with psychotropic medications (antidepressant or antipsychotic agents) can be predicted based on the assessment of serotonergic responsiveness prior to treatment. These data provide the impetus to develop an in vivo measure of central serotonergic activity with PET to evaluate etiologic and therapeutic mechanisms in neuropsychiatric disease. Future studies will be undertaken to evaluate the combination of [^{18}F]altanserin binding with pharmacologic challenges that directly and indirectly alter serotonin activity to evaluate the use of [^{18}F]altanserin as a potential dynamic measure of serotonin activity in vivo.

ACKNOWLEDGMENTS

We thank Marsha Dachille, Marybeth Wiseman, Lisa Hartman, Donna Milko, James Ruszkiewicz, Louise Smith, David Manthei, Blaise Blastos, Jennifer Perevuznik, and Kathie Antonnetti for their invaluable contributions to the PET studies. The CHO-5HT_{2A} cell line was provided by Kelly Berg of the Department of Pharmacology, University of Texas Health Science Center at San Antonio. Ruth Henteleff assisted in performing the binding assays. SR 46439B was generously provided by Sanofi-Winthrop.

REFERENCES

Arora, R., and Meltzer, H. (1991) Serotonin (5HT-2) receptor binding in the frontal cortex of schizophrenic patients. J. Neural Transm., 85:19–29.

Azmitia, E., and Gannon, P. (1986) The primate serotonergic system: A review of the human and animal studies and a report on the *Macaca fascicularis*. Adv. Neurol., 43:407–468.

Bartlett, E., Brodie, J., Wolf, A., Christman, D., Laska, E., and Meissner, M. (1988) Reproducibility of cerebral glucose metabolic measurements in resting human subjects. J. Cereb. Blood Flow Metab., 8:502–512.

Benloucif, S., Keegan, M., and Galloway, M. (1993) Serotonin-facilitated dopamine release *in vivo*: Pharmacological characterization. J. Pharmacol. Exp. Ther., 265:373–377.

Besret, L., Dauphin, F., Huard, C., Lasne, M., Vivet, R., Mickala, P., Barblieien, A., and Baron, J. (1996) Specific *in vivo* binding in the rat brain of [^{18}F]RP 62203: A selective 5-HT_{2A} receptor radioligand for positron emission tomography. Nucl. Med. Biol., 23:169–171.

Biver, F., Goldman, S., Luxen, A., Monclus, M., Forestini, M., Mendlewicz, J., and Lotstra, F. (1994) Multicompartmental study of fluorine-18 altanserin binding to brain 5-HT2 receptors in humans using positron emission tomography. Eur. J. Nucl. Med., 21:937–946.

Blin J., Pappata, S., Kiyosawa, M., Crousel, C., and Baron, J. (1988) [^{18}F]setoperone: A new high-affinity ligand for positron emission tomography study of the serotonin-2 receptors in the baboon brain in vivo. Eur. J. Pharmacol., 147:73–82.

Brown, G., and Linnoila, M. (1990) CSF serotonin metabolite (5-HIAA) studies in depression, impulsivity and violence. J. Clin. Psychiatry, 51:42–43.

Cross, A., Crow, T., Ferrier, I., and Johnson, J. (1986) The selectivity of the reduction of serotonin S2 receptors in Alzheimer-type dementia. Neurobiol. Aging, 7:3–7.

Dahlstrom, A., and Fuxe, D. (1984) Evidence for the existence of monoamine containing neurons in the central nervous system. Acta Physiol. Scand., 232:1–55.

Deutsch, A., Moghaddam, B., Innis, R., Krystal, J., Aghajanian, G., Bunney, B., and Charney, D. (1991) Mechanisms of action of atypical antipsychotic drugs. Schizophr. Res., 4:121–156.

Dewey, S., Macgregor, R., and Brodie, J. (1990) Mapping muscarinic receptors in the human and baboon brain using N-^{11}C-methylbenztropine. Synapse, 5:213–233.

Diksic, M., Nagahiro, S., Sourkes, T., and Yamamoto, Y. (1990) A new method to measure brain serotonin synthesis *in vivo*. I. Theory and basic data for a biological model. J. Cereb. Blood Flow Metab., 9:1–12.

Frost, J.J. (1990) Imaging the serotonin system by positron emission tomography. Ann. N.Y. Acad. Sci., 600:272–28.

Gross-Isseroff, R., Salama, D., Israeli, M., and Biegon, A. (1990) Autoradiographic analysis of age-dependent changes in serotonin 5-HT2 receptors of the human brain post-mortem. Brain Res., 519:223–227.

Herregodts, P., Ebinger, G., and Michotte, Y. (1991) Distribution of monoamines in human brain: Evidence for neurochemical heterogeneity in subcortical as well as in cortical areas. Brain Res., 542:300–306.

Hirano, H., Day, J., and Fibiger, H. (1995) Serotonergic regulation of acetylcholine release in rat frontal cortex. J. Neurochem., 65:1139–1145.

Hollander, E., DeCaria, C., Nitescu, A., Gully, R., Suckow, R., Cooper, T., Gorman, J., Klein, D., and Liebowitz, M. (1992) Serotonergic function in obsessive-compulsive disorder. Arch. Gen. Psychiatry, 49:21–28.

Hoyer, D., Clarke, D., Fozard, J., Hartig, P., Martin, G., Mylecharane, E., Saxena, P., and Humphrey, P. (1994) International Union of Pharmacology classification of receptors for 5-hydroxytryptamine (serotonin). Pharmacol. Rev., 46:157–203.

Huang, S., Hoffman, E., Phelps, M., and Kuhl, D. (1979) Quantitation in positron emission tomography. 2. Effects of inaccurate attenuation correction. J. Comput. Assist. Tomogr., 3:804–814.

Jones, B., and Cuello, A. (1989) Afferents to the basal forebrain cholinergic cell area from pontomesencephalic, catecholamine, serotonin and acetylcholine neurons. Neuroscience, 31:37–46.

Kahn, R., Davidson, M., Siever, L., Gabriel, S., Apter, S., and Davis, K. (1993) Serotonin function and treatment response to clozapine in schizophrenic patients. Am. J. Psychiatry, 150:1337–1342.

Leibowitz, S., and Shor-Posner, G. (1986) Serotonin and eating behavior. Appetite, 7:1–14.

Lemaire, C., Cantineau, R., Guillaume, M., Plenevaux, A., and Christians, L. (1991) Fluorine-18-altanserin: A radioligand for the study of serotonin receptors with PET: Radiolabeling and *in vivo* biologic behavior in rats. J. Nucl. Med., 32:2266–2272.

Leysen, J. (1989) Use of 5-HT$_2$ receptor agonists and antagonists for the characterization of their respective receptor sites. In: Drugs as Tools in Neurotransmitter Research. A. Boulton, C. Baker, and A. Juorio, eds. Humana, pp. 299–350.

Leysen, J. (1990) Gaps and peculiarities in 5-HT2 receptor studies. Neuropsychopharmacology, 3:361–369.

Logan, J., Fowler, J., Volkow, N., Wolf, A., Dewey, S., Schleyer, D., Macgregor, R., Hitzemann, R., Bendriem, B., Gatley, S., and Christman, D. (1990) Graphical analysis of reversible radioligand binding from time-activity measurements applied to N-^{11}C-methyl-(-)-cocaine PET studies in human subjects. J. Neurochem., 10:740–747.

Logan, J., Dewey, S., Wolf, A., Fowler, J., Brodie, J., Angrist, B., Volkow, N., and Gatley, J. (1991) Effects of endogenous dopamine on measures of ^{18}F-N-methylspiroperidol binding in the basal ganglia: Comparison of simulations and experimental results from PET studies in baboons. Synapse, 9:195–207.

Lopresti, B., Holt, D., Mason, N., Huang, Y., Ruszkiewicz, J., Perevuznik, J., Price, J., Smith, G., Mathis, C. (1998) Characterization of the radiolabelled metabolites of [^{18}F]-altanserin: Implications for kinetic modeling. In: Quantitative Brain Imaging with Positron Emission Tomography. R. Carson, M. Daube-Witherspoon, and P. Herscovitch, eds. Academic Press, New York pp 293–298.

Malone, K., Thase, M., Mieczkowski, T., Myers, J., Stull, S., Cooper, T., and Mann, J. (1993) Fenfluramine challenge test as a predictor of outcome in major depression. Psychopharmacol. Bull., 29:155–161.

Mann, J., Malone, K., Diehl, D., Perel, J., Cooper, T., and Mintun, M. (1996) Demonstration *in vivo* of reduced serotonin responsivity in the brain of untreated depressed patients. Am. J. Psychiatry, 153:174–182.

Mason, N.S., Huang, Y., Holt, D., Pervuznik, J., Lopresti, B., and Mathis, C. (1997) Synthesis of two radiolabelled metabolites of [^{18}F]-altanserin: [^{18}F]-3-[2-[4-(4-fluorophenylmethanol)-piperidinyl-]ethyl]-2–3-dihydro-2-thioxo-4-(1H)-quinazolidone and [^{18}F]4-(4-fluoro-benzoylpiperidine. J. Labeled Compounds Radiopharm., XL: 161–162.

Mathis, C., Simpson, N., Mahmood, K., Kinahan, P., and Mintun, M. (1994) [^{11}C]-WAY-100,635: A radioligand for imaging 5-HT1A receptors with positron emission tomography. Life Sci., 55:403–407.

Mathis, C., Mahmood, K., Huang, H., Simpson, N., Gerdes, J., and Price, J. (1996) Synthesis and preliminary *in vivo* evaluation of [^{11}C]MDL 100907: A potent and selective radioligand for the 5-HT$_{2A}$ receptor system. Med. Chem. Res., 6:1–10.

McCarley, R., and Hobson, J. (1975) Neuronal excitability modulation over the sleep cycle: A structural and mathematical model. Science, 189:58–60.

Meltzer, H. (1991) Serotonergic dysfunction in depression. Br. J. Psychiatry, 8:25–31.

Meuldermans, W., Hendrickx, J., Lauwers, W., Swysen, E., Hurkmans, R., Knaeps, E., Woestenborghs, R., and Heykants, J. (1984) Excretion and biotransformation of ketanserin after oral and intravenous administration in rats and dogs. Drugs Metab. Dispos., 12:772–781.

Minoshima, S., Berger, K., Lee, K., and Mintun, M. (1992) An automated method for rotational correction and centering of three-dimensional functional brain images. J. Nucl. Med., 33:1579–1585.

Morilak, D., Garlow, S., and Ciaranello, R. (1994a) Immunocytochemical localization and description of neurons expressing serotonin$_2$ receptor in the rat brain. Neuroscience, 54:701–717.

Morilak, D., Somogi, P., Lugan-Miras, R., and Ciaranello, R. (1994b) Neurons expressing serotonin$_2$ receptors in the rat brain: Neurochemical identification of cell types by immunohistochemistry. Neuropsychopharmacology, 11:157–166.

Parent, A., Descarries, L., and Beaudet, A. (1981) Organization of ascending serotonin systems in the adult rat brain. A radioautographic study after intraventricular administration of [^{3}H]5-hydroxytryptamine. Neuroscience, 6:115–138.

Pate, B., Snow, B., Hewitt, K., Morisson, S., Ruth, T., and Calne, D. (1991) The reproducibility of striatal uptake data obtained with positron emission tomography and fluorine-^{18}-L-6-fluorodopa tracer in non-human primates. J. Nucl. Med., 32:1246–1251.

Pazos, A., Cortes, R., and Palacios, J. (1985) Quantitative autoradiographic mapping of serotonin receptors in the rat brain. II. Serotonin$_2$ receptors. Brain Res., 346:231–249.

Pazos, A., Probst, A., and Palacios, J. (1987) Serotonin receptors in the human brain. IV. Autoradiographic mapping of serotonin$_2$ receptors. Neuroscience, 21:123–139.

Peroutka, S. (1994) Molecular biology of serotonin (5-HT) receptors. Synapse, 18:241–260.

Pike, V. (1995) Radioligands for PET studies of central 5-HT receptors and re-uptake sites—Current status. Nucl. Med. Biol., 22:1011–1018.

Price, J., Lopresti, B., Huang, Y., Holt, D., Smith, G., and Mathis, C. (1998) [^{18}F]-Altanserin PET studies of serotonin-2A binding: Examination of nonspecific binding component. In: Quantitative Brain Imaging with Positron Emission Tomography. R. Carson, M. Daube–Witherspoon, and P. Herscovitch, eds. Academic Press, New York pp 427–434.

Rinaldi-Carmona, M., Congy, C., Santucci, V., Simiand, J., Gautret, B., Neliat, G., Labeeuw, B., LeFur, G., Soubrie, P., and Breliere, J. (1992) Biochemical and pharmacological properties of SR 46349B, a new potent and selective 5-hydroxytryptamine$_2$ receptor antagonist. J. Pharmacol. Exp. Ther., 262:759–768.

Sadzot, B., Lemaire, C., Maquet, P., Salmon, E., Plenevaux, A., Degueldre, C., Hermanne, J., Guillaume, M., Cantineau, R., Comar, D., and Franck, G. (1995) Serotonin 5-HT$_2$ receptor imaging in the human brain using positron emission tomography and a new radioligand, [^{18}F]altanserin: Results in young, normal controls. J. Cereb. Blood Flow Metab., 15:787–797.

Spoont, M. (1992) Modulatory role of serotonin in neural information processing: Implications for human psychopathology. Psychiatr. Bull., 112:330–350.

Stahl, S., and Wets, K. (1987) Indoleamines and schizophrenia. In: Handbook of Schizophrenia, Vol. 2. F. Henn and L. deLisi, eds. pp. 257–296.

Steinbusch, H. (1981) Distribution of serotonin immunoreactivity in the central nervous system of the rat. Neuroscience, 6:557–618.

Strother, S.C., Anderson, J.R., Xu, X.L., Liow, J.S., Bonar, D.C., and Rottenberg, D.A. (1994) Quantitative comparisons of image registration techniques based on high-resolution MRI of the brain. J. Comput. Assist. Tomogr., 18:954–962.

Suehiro, M., Scheffel, U., Dannals, R., Ravert, H., Ricaute, G., and Wagner, H. (1993) A PET radiotracer for studying serotonin reuptake sites: Carbon-^{11}-McN-5652Z. J. Nucl. Med., 34:120–127.

Tan, P., Dewey, S., Gatley, S.J., Pappas, N., MacGregor, R., Ding, Y-S., Shea, C., Alexoff, D., Martin, T., Jenkins, D., King, P., Fowler, J., Ashby, C., and Wolf, A. (1994) Drug pharmacokinetics and pharmacodynamics: PET and microdialysis studies of SR 46349B, a selective 5-HT_2 antagonist. J. Nucl. Med., 35:67.

Van Bockstaele, E.J., Cestari, D.M., and Pickel, V.M. (1994) Synaptic structure and connectivity of serotonin terminals in the ventral tegmental area: Potential sites for modulation of mesolimbic dopamine neurons. Brain Res., 647:307–322.

Volkow, N., Fowler, J., Wang, G-J., Dewey, S., Schleyer, D., MacGregor, R.,Logan, J., Alexoff, D., Shea, C., Hitzeman, R., Angrist, B., and Wolf, A. (1993) Reproducibility of repeated measures of carbon-11 raclopride binding in the human brain. J. Nucl. Med., 34:609–613.

Wolf, W., and Kuhn, D. (1991) Cocaine and serotonin neurochemistry. Neurochem. Int., 18:33–38.

Woods, R.P., Cherry, S., and Mazziotta, J. (1992) Rapid automated algorithm for aligning and reslicing PET images. J. Comput. Assist. Tomogr., 16:620–633.

Woods, R.P., Mazziotta, J.C., and Cherry, S.R. (1993) MRI-PET registration with automated algorithm. J. Comput. Assist. Tomogr., 17:536–546.